

Comparing efficient computation methods for massless QCD tree amplitudes: Closed Analytic Formulae versus Berends-Giele Recursion

SIMON BADGER¹, BENEDIKT BIEDERMANN², LUCAS HACKL^{2,3},
JAN PLEFKA², THEODOR SCHUSTER² AND PETER UWER²

¹*The Niels Bohr International Academy and Discovery Center
The Niels Bohr Institute
Blegdamsvej 17, DK-2100 Copenhagen, Denmark*

²*Institut für Physik, Humboldt-Universität zu Berlin,
Newtonstraße 15, D-12489 Berlin, Germany*

³*Perimeter Institute for Theoretical Physics,
Waterloo, Ontario N2L 2Y5, Canada*

Abstract

Recent advances in our understanding of tree-level QCD amplitudes in the massless limit exploiting an effective (maximal) supersymmetry have led to the complete analytic construction of tree-amplitudes with up to four external quark-anti-quark pairs. In this work we compare the numerical efficiency of evaluating these closed analytic formulae to a numerically efficient implementation of the Berends-Giele recursion. We compare calculation times for tree-amplitudes with parton numbers ranging from 4 to 25 with no, one, two and three external quark lines. We find that the exact results are generally faster in the case of MHV and NMHV amplitudes. Starting with the NN-MHV amplitudes the Berends-Giele recursion becomes more efficient. In addition to the runtime we also compared the numerical accuracy. The analytic formulae are on average more accurate than the off-shell recursion relations though both are well suited for complicated phenomenological applications. In both cases we observe a reduction in the average accuracy when phase space configurations close to singular regions are evaluated. We believe that the above findings provide valuable information to select the right method for phenomenological applications.

Contents

| | | |
|----------|---|-----------|
| 1 | Introduction | 2 |
| 2 | Description of used methods | 4 |
| 2.1 | Closed analytic formulae | 4 |
| 2.2 | Berends-Giele recursion | 7 |
| 3 | Performance and Numerical Accuracy | 9 |
| 3.1 | Evaluation Time | 9 |
| 3.2 | Numerical Accuracy | 13 |
| 4 | Conclusions | 18 |

1 Introduction

Numerically fast and accurate computation methods for multi-parton tree-level amplitudes in QCD are of great importance from many points of view. They crucially enter the theoretical prediction for cross sections of multi-jet processes at leading order (LO) in the QCD coupling α_s as they occur at present particle colliders such as the Large Hadron Collider (LHC). Here a variety of computer programs based on the numerical evaluation of Feynman diagrams have been developed in the past see for example [1]. With the LHC data from the year 2011 jet multiplicities of up to 9 jets in the final state are probed. With the data of the year 2012, LHC will be able to investigate jet multiplicities of up to 12 jets. However, for high multiplicities, the conventional Feynman diagram based approach quickly reaches its limit, for example 8 jets in the final state would require already the evaluation of more than 10^7 Feynman diagrams! Hence more efficient methods are needed. Here important progress has been made in recent years based on recursive on-shell methods. Moreover, QCD tree-amplitudes are crucially needed for the computation of one-loop corrections, when these are constructed using a numerical implementation of generalized unitarity (for recent reviews see refs. [2]). Recently rapid progress has been made in developing and automating the generalized unitarity and integrand reduction approaches to computation of loop amplitudes [3,4]. These techniques have made NLO predictions for multi-jet final states at hadron colliders feasible for up to $2 \rightarrow 5$ processes (for recent results see for example [5]). On the formal side a number of new methods have been devised for the computation of scattering amplitudes in $SU(N_c)$ gauge theories with particular emphasis on the maximally supersymmetric ($\mathcal{N} = 4$) Yang-Mills theory. Among a host of other developments the Britto, Cachazo, Feng and Witten (BCFW) recursion relation [6] was developed which uses only on-shell lower-point amplitudes evaluated at complex momenta to construct the desired higher-point trees in any gauge theory. The BCFW recursion

was then recast as a super-recursion for super-amplitudes in the maximally supersymmetric case of ($\mathcal{N} = 4$) Yang-Mills theory [7]. This super-recursion could then be solved for arbitrary external states by Drummond and Henn in [8] leading to closed analytic formulae for all super-amplitudes at tree-level. The projection of the super-amplitudes on the component field level yielding $\mathcal{N} = 4$ super Yang-Mills theory amplitudes with external gluons, gluinos and scalars may be obtained upon suitable Grassmann integrations. This was done recently by Dixon, Henn and two of the present authors [9] who went on to show, that all primitive tree-amplitudes in massless QCD with up to four external quark lines of arbitrary flavors and an arbitrary number of gluons may be obtained from associated gluon-gluino trees in $\mathcal{N} = 4$ Yang-Mills theory. This result was then exploited to write down explicit analytic formulae for all tree-level amplitudes in massless QCD with up to four quark lines. Moreover, a publicly available MATHEMATICA package GGT was provided which generates all analytic tree-level gluon-gluino amplitudes relevant for QCD.¹ In its current version GGT directly provides all QCD tree amplitudes with up to six quarks. The obtained analytic formulae are very compact at the maximally-helicity-violating (MHV) and next-to-maximally helicity violating (NMHV) levels but do grow considerably in complexity with growing k for N^k MHV amplitudes.

Hence the “ $\mathcal{N} = 4$ SUSY method” [9] for the evaluation of massless QCD trees based on exact formulae displays a complementary situation to the conventional Berends-Giele recursive approach for the efficient numerical evaluation of trees in that its evaluation time scales mildly with the parton number n but strongly depends on the number of helicity flips k of the amplitude considered. In contrast the Berends-Giele recursion evaluation time is independent of k but strongly depends on the number of partons n . The purpose of this work is a detailed analysis of the computation times for these two approaches as well as a test of their numerical accuracy. The outcome of our analysis may serve as a guideline on which implementation should be used in order to maximally speed up the numerical implementation of massless QCD trees in future numerical calculations. The ability to calculate tree amplitudes numerically in a fast and accurate manner even for high multiplicity opens up a variety of new applications beyond the current uses in fixed order calculations. Given the recent progress in the refinement of matching and parton-shower algorithms together with extended reach of the LHC searches it is very likely that amplitudes involving ten or even more external partons will enter phenomenological studies in the future.

A similar analysis as presented in this paper has been performed in Refs. [11]. In difference to Refs. [11] we focus on the comparison of a purely numerical approach with the usage of analytic formulae, since this has not been studied in detail before. Furthermore we compare the numerical accuracy of the numerical approach with the numerical evaluation of analytic formulae. We also note that very recently the usage of Graphics Processing Units (GPUs) for the evaluation of tree-amplitudes has been investigated. More details on this interesting option can be found for example in Refs. [12].

¹A MATHEMATICA package for all tree-level amplitudes in $N=4$ SYM appeared in [10].

2 Description of used methods

Tree-level gluon amplitudes in non-abelian gauge theories may be conveniently separated into a sum of terms, each composed of a simple prefactor containing the color indices, multiplied by a kinematical factor known as a partial or color-ordered amplitude. For an n -gluon amplitude one has

$$\mathcal{A}_n^{\text{tree}}(1, 2, 3, \dots, n) = g^{n-2} \sum_{\sigma \in \mathcal{S}_n / Z_n} \text{Tr}(T^{a_{\sigma(1)}} \dots T^{a_{\sigma(n)}}) A_n(\sigma(1)^{h_{\sigma(1)}} \dots \sigma(n)^{h_{\sigma(n)}}), \quad (1)$$

with the argument i^{h_i} of the partial amplitude A_n denoting an outgoing gluon of light-like momentum p_i and helicity $h_i = \pm 1$, $i \in [1, n]$. The $su(N_c)$ generator matrices T^{a_i} are in the fundamental representation, and are normalized so that $\text{Tr}(T^a T^b) = \delta^{ab}$. Finally, g is the gauge coupling.

Similarly, the color decomposition of an amplitude with a single quark-anti-quark pair and $(n-2)$ gluons is

$$\mathcal{A}_n^{\text{tree}}(1_{\bar{q}}, 2_q, 3, \dots, n) = g^{n-2} \sum_{\sigma \in \mathcal{S}_{n-2}} (T^{a_{\sigma(3)}} \dots T^{a_{\sigma(n)}})_{i_2}^{\bar{i}_1} A_n^{\text{tree}}(1_{\bar{q}}, 2_q, \sigma(3), \dots, \sigma(n)). \quad (2)$$

Amplitudes with two and more quark-anti-quark lines may be obtained similarly, as explained in ref. [13]. Though the color structure becomes more intricate in these cases, all of the required kinematical terms are constructed from suitable linear combinations of the color-ordered amplitudes for $2k$ external gluinos and $(n-2k)$ external gluons.

Color-ordered amplitudes of massless particles are most compactly expressed in the spinor-helicity formalism. Here all light-like four-momenta are written as the product of two component Weyl spinors

$$p^{\mu} = \sigma_{\mu}^{\alpha\dot{\alpha}} p^{\mu} = \lambda^{\alpha} \tilde{\lambda}^{\dot{\alpha}}, \quad (3)$$

where we take $\sigma^{\mu} = (\mathbf{1}, \vec{\sigma})$ with $\vec{\sigma}$ being the 2×2 Pauli spin matrices. The spinor indices are raised and lowered with the Levi-Civita tensor, i.e. $\lambda_{\alpha} = \epsilon_{\alpha\beta} \lambda^{\beta}$ and $\tilde{\lambda}_{\dot{\alpha}} = \epsilon_{\dot{\alpha}\dot{\beta}} \tilde{\lambda}^{\dot{\beta}}$. An explicit representation is

$$|\lambda\rangle := \lambda_{\alpha} = \frac{\sqrt{p^0 + p^3}}{p^1 - ip^2} \begin{pmatrix} p^1 - ip^2 \\ p^0 - p^3 \end{pmatrix}, \quad |\tilde{\lambda}] := \tilde{\lambda}^{\dot{\alpha}} = \frac{\sqrt{p^0 + p^3}}{p^1 + ip^2} \begin{pmatrix} -p^0 + p^3 \\ p^1 + ip^2 \end{pmatrix}. \quad (4)$$

In our convention all parton momenta are outgoing. The amplitudes depend on contracted helicity spinors

$$\langle i j \rangle := \langle \lambda_i \lambda_j \rangle := \epsilon_{\alpha\beta} \lambda_i^{\alpha} \lambda_j^{\beta}, \quad [i j] := [\tilde{\lambda}_i \tilde{\lambda}_j] := \epsilon_{\dot{\alpha}\dot{\beta}} \tilde{\lambda}_i^{\dot{\alpha}} \tilde{\lambda}_j^{\dot{\beta}}, \quad (5)$$

which are Lorentz invariants.

2.1 Closed analytic formulae

Compact analytic formulae for tree-amplitudes in the spinor helicity formalism can be classified by the amount of helicity violation. The simplest class is the maximally-helicity-violating

(MHV) one. Here either two negative helicity gluons, one negative helicity gluon and one quark-anti-quark pair or two quark-anti-quark pairs sit at arbitrary positions within positive helicity gluon states of the color-ordered amplitude. These read for the zero and one fermion line case [14, 13]

$$A_n^{\text{MHV}}(a^-, b^-) = \delta^{(4)}(p) \frac{\langle a b \rangle^4}{\langle 1 2 \rangle \langle 2 3 \rangle \dots \langle n 1 \rangle} \quad (6)$$

$$A_n^{\text{MHV}}(a^-, b_q, c_{\bar{q}}) = \delta^{(4)}(p) \frac{\langle a c \rangle^3 \langle a b \rangle}{\langle 1 2 \rangle \dots \langle n 1 \rangle}, \quad (7)$$

$$A_n^{\text{MHV}}(a^-, b_{\bar{q}}, c_q) = -\delta^{(4)}(p) \frac{\langle a b \rangle^3 \langle a c \rangle}{\langle 1 2 \rangle \dots \langle n 1 \rangle}, \quad (8)$$

where $a, b, c \in [1, n]$ and a^- denotes a negative-helicity gluon at position a , while fermions of opposite helicity with flavors A, B at positions b, c are denoted by b_q^A ($+\frac{1}{2}$) and $c_{\bar{q}}^B$ ($-\frac{1}{2}$), and $p = \sum_{i=1}^n p_i$. Flavor becomes important for the two fermion line case where one has three distinct representatives depending on helicity and flavor distributions [9]

$$A_n^{\text{MHV}}(a_q^1, b_q^2, c_{\bar{q}}^2, d_{\bar{q}}^1) = -\delta^{(4)}(p) \frac{\langle c d \rangle^3 \langle a b \rangle}{\langle 1 2 \rangle \dots \langle n 1 \rangle} = A_n^{\text{MHV}}(a_q, b_q, c_{\bar{q}}, d_{\bar{q}}), \quad (9)$$

$$A_n^{\text{MHV}}(a_q^1, b_{\bar{q}}^1, c_q^2, d_{\bar{q}}^2) = \delta^{(4)}(p) \frac{\langle b d \rangle^2 \langle d a \rangle \langle c b \rangle}{\langle 1 2 \rangle \dots \langle n 1 \rangle}, \quad (10)$$

$$A_n^{\text{MHV}}(a_q, b_{\bar{q}}, c_q, d_{\bar{q}}) = \delta^{(4)}(p) \frac{\langle b d \rangle^3 \langle a c \rangle}{\langle 1 2 \rangle \dots \langle n 1 \rangle}, \quad (11)$$

where the flavor index has been omitted in the single flavor cases.

The complexity of the closed formulae grows at the NMHV level comprising color-ordered amplitudes with k negative helicity gluons and $3 - k$ quark-anti-quark pairs embedded in a sea of $(n + k - 6)$ positive helicity gluon states. In order to express the formulae in a compact way one needs to introduce the region momenta $x_{ij}^{\alpha\dot{\alpha}}$ via

$$x_{ij}^{\alpha\dot{\alpha}} := (\not{p}_i + \not{p}_{i+1} + \dots + \not{p}_{j-1})^{\alpha\dot{\alpha}} = \sum_{k=i}^{j-1} \lambda_k^\alpha \tilde{\lambda}_k^{\dot{\alpha}}, \quad i < j, \quad (12)$$

$x_{ii} = 0$, and $x_{ij} = -x_{ji}$ for $i > j$. All $N^k\text{MHV}$ tree-level amplitudes can be expressed in terms of the quantities $\langle na_1 a_2 \dots a_k | a \rangle$ defined by

$$\langle na_1 a_2 \dots a_k | a \rangle := \langle n | x_{na_1} x_{a_1 a_2} \dots x_{a_{k-1} a_k} | a \rangle, \quad (13)$$

and the spinor products $\langle i j \rangle$. The pure gluon NMHV amplitude with negative helicity gluons sitting at positions a, b and n takes the form [9]

$$A_n^{\text{NMHV}}(a^-, b^-, n^-) = \frac{\delta^{(4)}(p)}{\langle 1 2 \rangle \dots \langle n 1 \rangle} \times$$

$$\left[\sum_{a < s \leq b < t \leq n-1} \tilde{R}_{n,st} \left(\langle n a \rangle \langle nts|b \rangle \right)^4 + \sum_{a < s < t \leq b} \tilde{R}_{n,st} \left(\langle b n \rangle \langle n a \rangle x_{st}^2 \right)^4 \right. \\ \left. + \sum_{2 \leq s \leq a < b < t \leq n-1} \tilde{R}_{n,st} \left(\langle b a \rangle \langle nts|n \rangle \right)^4 + \sum_{2 \leq s \leq a < t \leq b} \tilde{R}_{n,st} \left(\langle n b \rangle \langle nst|a \rangle \right)^4 \right], \quad (14)$$

where we have introduced the \tilde{R} -invariant

$$\tilde{R}_{n,st} := \frac{1}{x_{st}^2} \frac{\langle s(s-1) \rangle}{\langle nts|s \rangle \langle nts|s-1 \rangle} \frac{\langle t(t-1) \rangle}{\langle nst|t \rangle \langle nst|t-1 \rangle}. \quad (15)$$

with $\tilde{R}_{n,st} := 0$ for $t = s + 1$ or $s = t + 1$. Let us also state NMHV amplitude with one quark-anti-quark pair and two negative-helicity gluons. Here there are two distinct configurations (we take $a < b < c$ below) [9]

$$A_n^{\text{NMHV}}(a_q, b^-, c_{\bar{q}}, n^-) = \frac{\delta^{(4)}(p)}{\langle 1 2 \rangle \dots \langle n 1 \rangle} \left[-\langle a b \rangle \langle b c \rangle^3 \sum_{1 < s \leq a, b, c < t < n} \langle nts|n \rangle^4 \tilde{R}_{n,st} \right. \\ - \langle b c \rangle^3 \langle a n \rangle \sum_{a < s \leq b, c < t < n} \langle nts|b \rangle \langle nts|n \rangle^3 \tilde{R}_{n,st} \\ - \langle c n \rangle^3 \langle a n \rangle \sum_{a < s \leq b < t \leq c} \langle nst|b \rangle^3 \langle nts|b \rangle \tilde{R}_{n,st} \\ \left. - \langle c n \rangle^3 \langle a b \rangle \sum_{1 < s \leq a, b < t \leq c} \langle nst|b \rangle^3 \langle nts|n \rangle \tilde{R}_{n,st} \right], \quad (16)$$

$$A_n^{\text{NMHV}}(a_q, b_{\bar{q}}, c^-, n^-) = \frac{\delta^{(4)}(p)}{\langle 1 2 \rangle \dots \langle n 1 \rangle} \left[+ \langle a c \rangle \langle b c \rangle^3 \sum_{1 < s \leq a, b, c < t < n} \langle nts|n \rangle^4 \tilde{R}_{n,st} \right. \\ + \langle a n \rangle \langle b n \rangle^3 \sum_{b < s \leq c < t < n} \langle nts|c \rangle^4 \tilde{R}_{n,st} \\ + \langle n c \rangle^4 \langle a n \rangle \langle b n \rangle^3 \sum_{b < s < t \leq c} (x_{st}^2)^4 \tilde{R}_{n,st} \\ + \langle c n \rangle^4 \sum_{1 < s \leq a, b < t \leq c} \langle nst|b \rangle^3 \langle nst|a \rangle \tilde{R}_{n,st} \\ + \langle b c \rangle^3 \langle a n \rangle \sum_{a < s \leq b, c < t < n} \langle nts|c \rangle \langle nts|n \rangle^3 \tilde{R}_{n,st} \\ \left. + \langle c n \rangle^4 \langle a n \rangle \sum_{a < s \leq b < t \leq c} x_{st}^2 \langle nst|b \rangle^3 \tilde{R}_{n,st} \right]. \quad (17)$$

The two and three fermion line amplitudes are more involved and may be found in the appendix B of [9]. These formulae have also been implemented in the publicly available MATHEMATICA package GGT². As already stated in the introduction, the current version of GGT also provides all QCD amplitudes with up to six quarks.

An estimate for the evaluation time of these closed formulae for the amplitudes is the number of terms the expression has. From this one estimates the evaluation time of the MHV amplitudes to be of order n since the number of spinor products to be evaluated is approximately n . The number of terms in the formulae for the NMHV amplitudes grows as n^2 for large parton numbers n . Excluding the MHV prefactor the complexity of each of the terms is independent of the parton number, hence the asymptotic scaling in evaluation time is n^2 . This is competitive with the Berends-Giele recursion method which grows independent on the helicity distributions of the partons as n^4 , discussed in the next subsection. The NNMHV formulae of [9] display a growth in the number of terms as n^4 . Due to the same arguments as in the NMHV case we thus expect a similar performance of the NNMHV formulae as the Berends-Giele recursion and a detailed comparison is needed to see which method wins. Going beyond the NNMHV level with the analytic formulae of [9] for the amplitudes appears to be disfavored as in general the number of terms in an N^k MHV formula grows as n^{2k} for large parton numbers.

The closed analytic formulae of [9] for the MHV, NMHV and NNMHV with zero to three quark-anti-quark lines have been directly implemented in a C++ program `cGGT.cpp` which can be provided upon request. `cGGT.cpp` contains the straightforwardly hard-coded analytic formulae and a natural amount of caching is performed in order to speed up the numerical evaluation of the amplitudes for a given phase-space point. As such all the region momenta are evaluated and stored during initialization, similarly all spinor brackets are evaluated with the reduced spinors in Eq. (4) without the square root dependent pre-factor, which is only evaluated at the very end, as typically even powers of the pre-factor arise.

2.2 Berends-Giele recursion

In this subsection we briefly comment on a purely numerical implementation of leading-order scattering amplitudes in massless QCD. Since an extensive literature exists on the subject we limit ourselves to the basic ingredients. More details can be found in Ref. [15]. In difference to on-shell recurrence relations developed more recently [6], the Berends-Giele recursion uses off-shell currents as basic building blocks. In pure gauge theory the off-shell currents $J_\mu(1^{h_1}, 2^{h_2}, \dots, n^{h_n})$ correspond to the amplitudes for the production of n gluons with helicities h_i and one off-shell gluon with the corresponding polarization vector stripped off. The on-shell scattering amplitude is thus obtained by taking the on-shell limit and contracting with the polarization vector of the additional gluon. As mentioned in the previous section it is convenient to split the scattering amplitude into a color part and the remaining Lorentz structure. In practice this can be done for example by using color-ordered Feynman rules (for details we refer to Ref. [16]). The full amplitude will in general contain different color structures. However since not all of these structures are independent it is usually sufficient to calculate

²Included in this submission and at <http://qft.physik.hu-berlin.de>

only a few of them and reconstruct the remaining ones by permuting the external gluons. The key observation leading to the Berends-Giele recurrence relation is the fact that any off-shell current can be written as a sum of simpler off-shell currents connected via the appropriate three- (V_{3g}) and four-gluon (V_{4g}) vertices:

$$J_\mu(1, \dots, n) = \frac{-i}{P_{i,n}^2} \left[\sum_{i=1}^{n-1} V_{3g}^{\mu\nu\rho}(P_{1,i}, P_{i+1,n}) J_\nu(1, \dots, i) J_\rho(i+1, \dots, n) \right. \\ \left. + \sum_{j=i+1}^{n-1} \sum_{i=1}^{n-2} V_{4g}^{\mu\nu\rho\sigma} J_\nu(1, \dots, i) J_\rho(i+1, \dots, j) J_\sigma(j+1, \dots, n) \right] \quad (18)$$

where we have suppressed the helicity index and the gauge coupling is set to one. In addition the definition

$$P_{i,j} = \sum_{k=i}^j p_k \quad \text{for } j \geq i \quad (19)$$

is used, we note $P_{i,j} = x_{i,j+1}$ from (12). The color-ordered vertices are given by

$$V_{3g}^{\mu\nu\rho}(P_1, P_2) = \frac{i}{\sqrt{2}} (g^{\nu\rho}(P_1 - P_2)^\mu + 2g^{\rho\mu}P_2^\nu - 2g^{\mu\nu}P_1^\rho), \\ V_{4g}^{\mu\nu\rho\sigma} = \frac{i}{2} (2g^{\mu\rho}g^{\nu\sigma} - g^{\mu\nu}g^{\rho\sigma} - g^{\mu\sigma}g^{\nu\rho}). \quad (20)$$

Since the right hand side of Eq. (18) is formally simpler—only off-shell currents with a lower number of gluons are involved—Eq. (18) can be used to calculate off-shell currents recursively. The end-point of the recursion is given by

$$J_\mu(i^{h_i}) = \left(\epsilon_\mu^{(h_i)}(p_i) \right)^* \quad (21)$$

where $\epsilon_\mu^{(h_i)}(p_i)$ denotes the polarization vector of a gluon with momentum p_i and polarization h_i . We take all the partons as outgoing, that is the on-shell limit of the scattering amplitudes correspond to the transition $0 \rightarrow g(1^{h_1}) \dots g(n^{h_n}) g((n+1)^{h_{n+1}})$. Scattering amplitudes for physical processes are obtained as usual by crossing. Using the explicit form of the three- and four-point vertices as given above, the implementation of Eq. (18) in a computer program is straight forward. As can be seen from Eq. (18) the same sub-current may appear at different depths of the recursion. To speed up the numerical evaluation it is thus important to cache the sub-currents and evaluate them only once. We note that the possibility to reuse sub-currents during the calculation is a major advantage of off-shell recurrence relations compared to on-shell methods. Since recursive implementations tend to be sub-optimal to get high computing performance Eq. (18) is implemented as a bottom-up approach. The program uses the one-point currents specified by the user in terms of particular polarization states together with the respective momenta to calculate the two-gluon off-shell currents $J_\mu(i^{h_i}, (i+1)^{h_{i+1}})$. The two-point currents together with the one-point currents are then used in the subsequent step to calculate the three-point currents. This procedure is repeated until the current of maximal length is obtained. Owing to our restriction to specific color structures only a fixed cyclic ordering needs to be considered. One can show that if sub-currents are cached the computational

effort for the evaluation of an n -point current scales as n^4 . (Without cache the scaling would be 4^n .) We will come back to this point when we discuss the numerical performance. As a technical detail we remark that in the implementation presented here [3] no specific bases for the polarization vectors has been used. In particular no helicity methods have been applied. Since in (almost) all phenomenological applications the gluon polarization is not observed, only matrix elements squared summed over all polarization states will occur. As a consequence an arbitrary bases can be used as long as the sum over all possible polarization states is complete. Using real polarization vectors could thus yield a significant speed up since the entire calculation can be done using real numbers instead of complex arithmetic.

The extension to include also quarks—massive as well as massless ones—is straight forward. The main difference, namely that some sub-currents do not exist since there is no direct coupling between quarks, is merely a matter of bookkeeping. We stress that the quark currents calculated in the way described above in general do not correspond to partial amplitudes. However partial amplitudes can be constructed from the aforementioned currents. The reconstruction of the full matrix elements—not subject of this article—has been checked for a variety of different processes [17].

3 Performance and Numerical Accuracy

The scattering amplitudes described in the previous section find their application in leading-order phenomenology at hadron colliders. However, this is not the only application. With the development of unitarity inspired techniques, leading-order amplitudes represent an important input to the evaluation of one-loop amplitudes. In both cases the amplitudes need to be evaluated for millions of phase space points. The required computation time is thus an important factor in choosing the optimal approach. We compare the evaluation time in detail in Section 3.1.

In particular when using leading-order amplitudes in the evaluation of one-loop amplitudes, not only the speed but also the numerical accuracy matters. In the unitarity method the one-loop amplitude is reconstructed from a large number of different cuts requiring the evaluation of the corresponding tree amplitudes. It is thus important to assure a good accuracy of the individual contributions. Even in the case that analytic formulae are available one should keep in mind that when it comes to the numerical evaluation usually only a finite floating point precision is employed — unless special libraries to allow for extended precision are used. As a consequence, numerical cancellations between individual contributions may result in a loss of accuracy of the final result. Since a detailed understanding of the numerical uncertainties is also important when results from different methods are compared we investigate the numerical uncertainties of the two approaches discussed in the previous Section in Section 3.2.

3.1 Evaluation Time

Before discussing the results in detail we briefly describe how the runtime is analyzed. To investigate the performance we used a computer with 16 GByte main memory and Intel(R) Core(TM) i5 3.33GHz cpu running under Debian 6.04. To reduce context switches as much

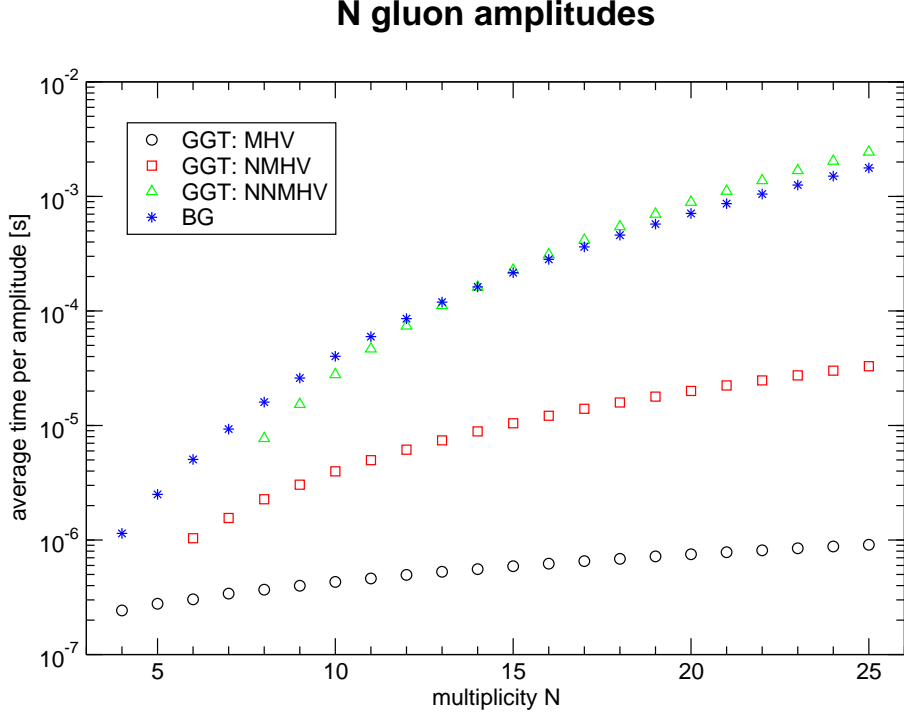


Figure 1: Average time required per phase space point for the evaluation of pure gluon amplitudes as function of the parton multiplicity.

as possible we paid attention to the fact that the computer was used exclusively for the performance measurements. Furthermore we used the POSIX function `getrusage` for the measurement of the used cpu time, which is to some great extent context independent. The function returns the time spent in user mode split into seconds and micro seconds. It is not documented whether the underlying clock provides a real time accuracy at the level of micro seconds. One can assume however that a precision at the level of milli seconds should be feasible which is sufficient for our purpose using the procedure described in the following.

The key observation is that both the evaluation time of the analytical formulae and of the Berends-Giele recursion depend on the positions of the fermions. In the case of the analytical formulae we additionally have a dependence on the position of the negative helicity gluons. Hence, we chose to average over all configurations to which the analytical formulae directly apply without exploiting the cyclic symmetry of the amplitudes, e.g. all configurations with a negative helicity gluon at position n for amplitudes with at least one gluon of negative helicity. To obtain reproduceable results and to reduce the computational effort to a minimum we took the following approach: Per measurement a minimum cpu time of at least one second is required to obtain reliable results. Using empirical knowledge together with the known scaling of the runtime as a function of the multiplicity we estimated the number of phase space evaluations for each sub-process/multiplicity. We then generated one phase space point and

evaluated all matrix elements corresponding to our desired average the required number of times. While in the determination of the accuracy it is important that on-shell condition and four momentum conservation are respected as precise as possible, the runtime measurement is insensitive to the “quality” of the phase space point—as long as no floating exceptions are encountered. (Floating point exceptions would lead to exception handling and the execution of different code.) In Fig. 1 the cpu time per phase space point for pure gluon amplitudes is shown. We compare analytic formulae for three different helicity configurations (MHV, NMHV, NNMHV) with the purely numerical approach using the Berends-Giele recursion. Since in the implementation of the Berends-Giele recursion no helicity methods are used the runtime is the same for different helicity configurations. Fitting the last five data points with $f(n) = An^B$, where n is the gluon multiplicity, we obtain $B \approx 4.12$ which is already quite close to the predicted asymptotic $O(n^4)$ behavior. We stress that this is a property of the algorithm and cannot be changed by a different implementation. The implementation can only affect the normalization factor in front of the n^4 behavior. Let us now compare with the runtime required for the evaluation of the analytic formulae. In case of the MHV amplitude the evaluation is more than three orders of magnitude faster for 25 gluons—as one would have expected given the compactness of the analytic results. We have checked that the timings shown for the MHV amplitudes perfectly agree with the predicted n^1 scaling. We emphasize that no time consuming square roots (contained in the spinor products) have to be evaluated in all gluon amplitudes since each spinor appears an even number of times. This is no longer true for amplitudes involving fermions as their associated spinors appear an odd number of times. Hence, for each fermion one square root is required. The predicted large n behavior of n^2 for the NMHV amplitudes is in good agreement with the $n^{2.2}$ fit from the last five data points in Fig. 1. This is still much better than the n^4 of the Berends-Giele approach. As a consequence for large multiplicities the analytic results are almost two orders of magnitude faster than Berends-Giele. The situation changes when it comes to the NNMHV amplitudes. From the number of terms in the analytic expression we expect an asymptotic behavior of the form n^4 leading to a similar rise of the runtime as a function of the gluon multiplicity as observed in the Berends-Giele case. However, fitting the last five data points reveals that, with a scaling of $n^{4.5}$ the analytic formulae are still farther away from the asymptotic behavior than Berends-Giele. Consequently for 15 gluons and more the Berends-Giele recursion starts to become more efficient. As mentioned already, the asymptotic behavior is a property of the underlying algorithm and cannot be changed by a ‘more clever’ implementation.

Let us add at that point a remark concerning the absolute timings: For low multiplicities the evaluation time is of the order of micro seconds while for $n = 25$ order milli seconds are required. For practical applications one should keep in mind, that the timings are for specific color and spin configurations. While for low multiplicities the number of color and spin configurations is still small (i.e. for $n \leq 5$ only MHV amplitudes exist) one can expect that color and spin summed squared amplitudes can be evaluated in less than one milli second per phase space point. However for large multiplicities the number of color and spin configurations grows rapidly. A naive sum over color and spin would thus give an additional factor which would render a brute force evaluation impossible given today’s computing resources. In such cases refined methods like for example Monte Carlo sums over spins and colors would be required.

(N-2) gluon 2 quark amplitudes

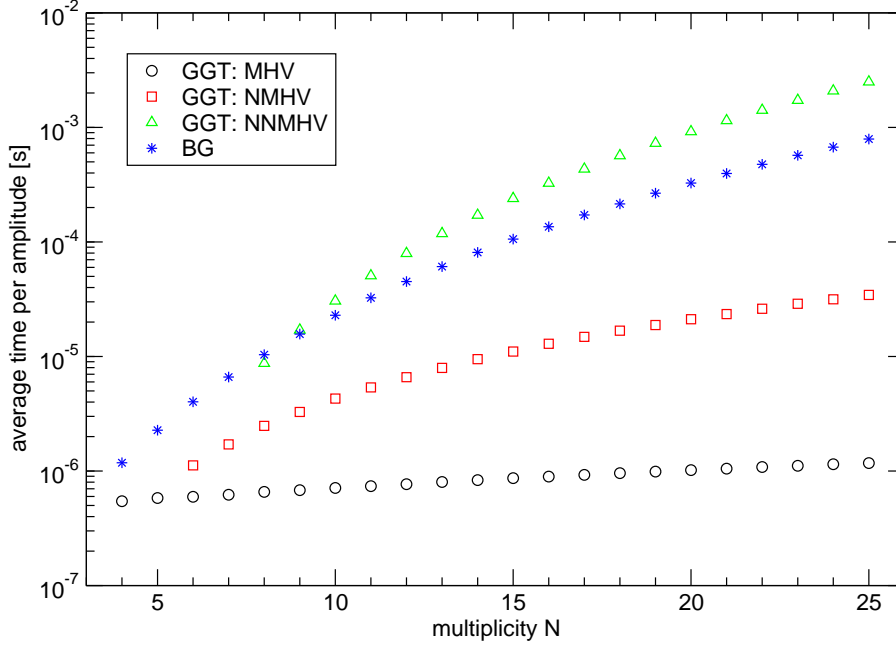


Figure 2: Evaluation time per phase space point for amplitudes with a quark–anti-quark pair and $N - 2$ gluons.

In Fig. 2, Fig. 3 and Fig. 4 we show the results of a similar analysis, now for amplitudes involving up to three quark–anti-quark pairs. Again the Berends-Giele recursion method is presented only for a fixed number of negative helicity gluons since our implementation is independent of the gluon helicities. However, to take into account that the runtime depends on the position of the quarks in the primitive amplitude we took the same configuration average as for the corresponding analytic formula of smallest MHV degree. Overall we observe a picture similar to the pure gluon case: for MHV and NMHV amplitudes the analytic results are much faster than the evaluation based on the Berends-Giele recursion. Comparing the performance of the Berends-Giele recursion for 0, 2, 4, 6 quarks we find a decreasing dependence on the parton multiplicity. This is simply due to the fact that for a fixed multiplicity the number of currents which have to be evaluated decreases if more fermions are involved. Since the n^4 asymptotic of the recursion is due to the four gluon vertex, we expect that the asymptotic scaling will be approached from below. Indeed, for two, four, six quarks we get $n^{3.96}$, $n^{3.83}$, $n^{3.64}$ from the last five data points compared to $n^{3.77}$, $n^{3.43}$, $n^{3.19}$ for up to $n = 15$ partons. The timings of the analytical formulae show only a small dependence on the number of quarks. As a consequence the Berends-Giele recursion is more efficient for the NNMHV amplitudes involving quarks. In case of all MHV amplitudes it is remarkable that the analytic formulae for MHV amplitudes show a very weak dependence on the parton multiplicity. The evaluation

(N-4) gluon 4 quark amplitudes

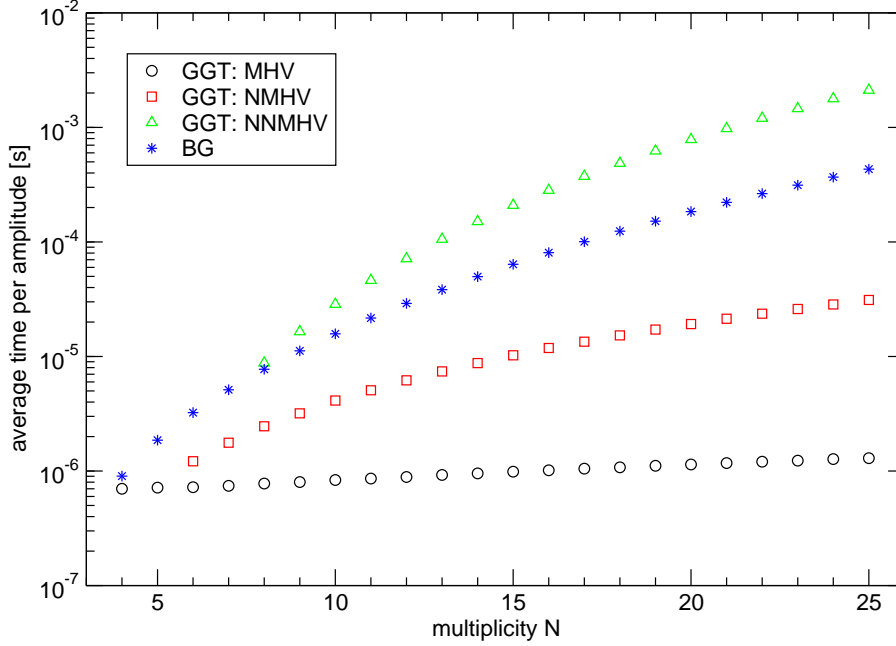


Figure 3: Evaluation time per phase space point for amplitudes with two quark–anti-quark pairs (different flavors) and $N - 4$ gluons.

of an MHV amplitude for $n = 25$ takes only $6 \times 10^{-7}s$ longer than the evaluation of the four point amplitude. This is easily understood from the structure of formulae since increasing the multiplicity by one results only in the additional evaluation of two reduced spinor products and one squared spinor normalization factor.

3.2 Numerical Accuracy

Understanding the numerical accuracy is crucial for numerical cross section evaluations. In cases where analytic results are available it is possible to assess the accuracy of purely numerical approaches by comparing with analytic results. However the numerical evaluation of analytic formulae may also be affected by numerical instabilities. Furthermore a reliable method is also required for situations where no analytic results are available. In [3] the so-called scaling test was proposed. When applying the scaling test the scattering amplitudes are calculated twice for a given phase space point: for each phase space point the scattering amplitudes are calculated for the given momentum configuration. The evaluation is then repeated for a re-scaled set of momenta. Since the corresponding effective operators are not renormalized no anomalous dimension appears. The two evaluations are thus related by their

(N-6) gluon 6 quark amplitudes

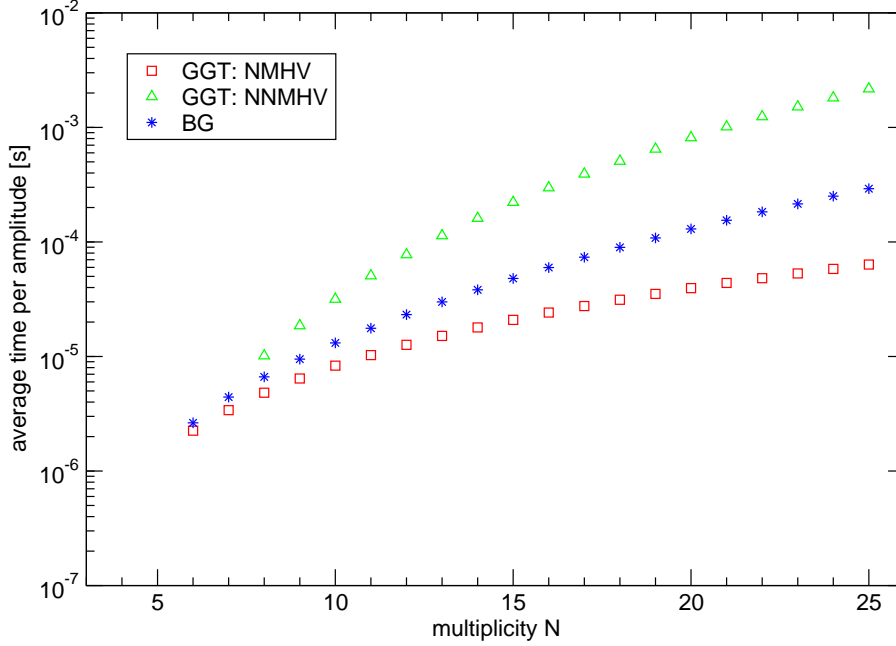


Figure 4: Evaluation time per phase space point for amplitudes with three quark–anti-quark pairs (different flavors) and $N - 6$ gluons.

naive mass dimension:

$$A_n(p_1, p_2, \dots, p_n) = x^{n-4} A_n(xp_1, xp_2, \dots, xp_n). \quad (22)$$

As was pointed out in [3] using a value for x which is not a power of 2 will lead to a different mantissa in the floating point representation and thus to different numerics. The method thus allows to assess the size of rounding errors. To estimate the numerical uncertainties we have applied the scaling test for a large number of phase space points. As a measure for the uncertainty we have evaluated for each phase space point the quantity δ :

$$\delta = \log_{10} \left(2 \left| \frac{A_1 - A_2}{A_1 + A_2} \right| \right), \quad (23)$$

where A_1 denotes the result of the amplitude evaluation for unscaled momenta while A_2 is calculated from Eq. (22). The quantity $|\delta|$ gives a measure for the valid digits in the evaluation, i.e. a value of $|\delta| = 3$ would mean that we expect ~ 3 digits to be correct. As an example we show in Fig. 5 results for the 25 gluon amplitude. In case of the Berends-Giele recursion the alternating helicity configuration $+-+ - + \dots$ is evaluated. The remaining three histograms show results using analytic formulae for MHV, NMHV, and NNMHV amplitudes. The phase space points are generated using a sequential splitting algorithm as described in [18]. This algorithm does not produce a flat distribution in phase space. In fact collinear configurations are

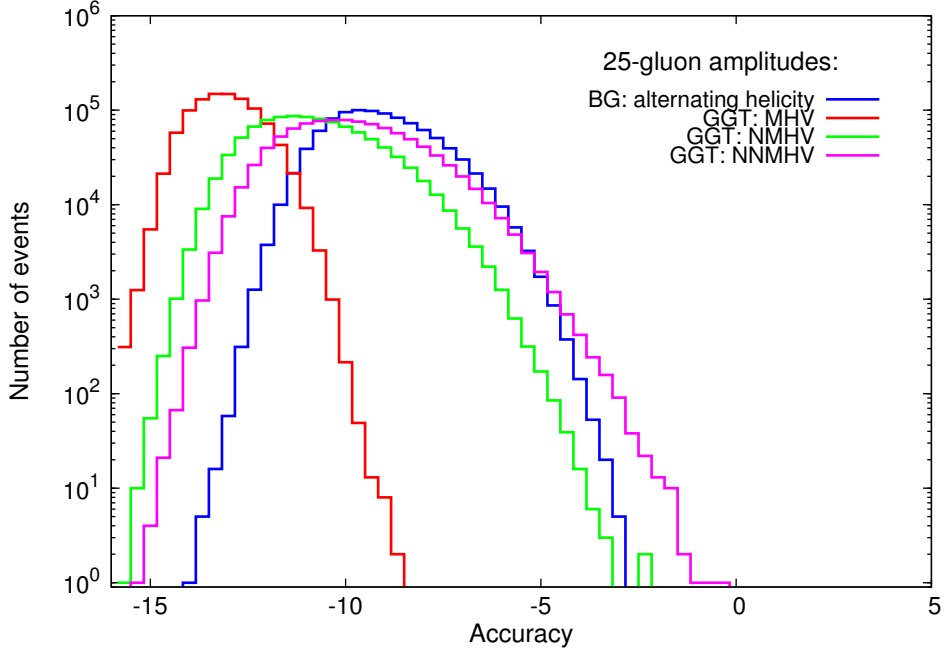


Figure 5: Accuracy δ for 25 gluon amplitude for purely numerical evaluation based on the Berends-Giele recursion (BG) and for analytic formulae (GGT) as described in Section 2.1. Phase-space generation by sequential splitting.

preferred. We note that we always use a couple of default cuts based on the JADE jet algorithm to avoid singular regions in the phase space. In particular we require $(2p_i \cdot p_j)/s > 10^{-10}$. We emphasize that as a consequence of the sequential splitting algorithm collinear configurations will dominate for multiplicities greater than 15, e.g. for $N = 20$ almost all phase space points have a collinearity of 10^{-10} . It follows from Fig. 5 that most of the phase space points are evaluated with a precision better than 5 valid digits—largely sufficient for any practical application at hadron colliders. Since we are mainly interested in a comparison between the purely numerical approach and the usage of analytic formulae for different parton multiplicities we have calculated an average accuracy for different parton multiplicities and different helicity configurations. The result is shown in Fig. 6. First of all we observe that in general the analytic formulae perform better as far as the accuracy is concerned. Furthermore it can be seen that for the analytic formulae the accuracy degrades when we move to the more complex configurations as for example the NNMHV amplitudes. This has two reasons. First of all the corresponding formulae are more involved and are thus more difficult to evaluate numerically. The second reason is due to numerical cancellations between individual terms which leads to a loss of accuracy. This is supported by the observation that the NNMHV split helicity where no cancellation occurs is almost as accurate as the MHV formula. In the worst case the accuracy is only marginally better than what we observe in the purely numerical case. For the Berends-Giele recurrence relations we show only one helicity configuration since no helicity methods are used as mentioned in the previous section. Describing the gluon polarization using a four-

Numerical precision of N gluon amplitudes

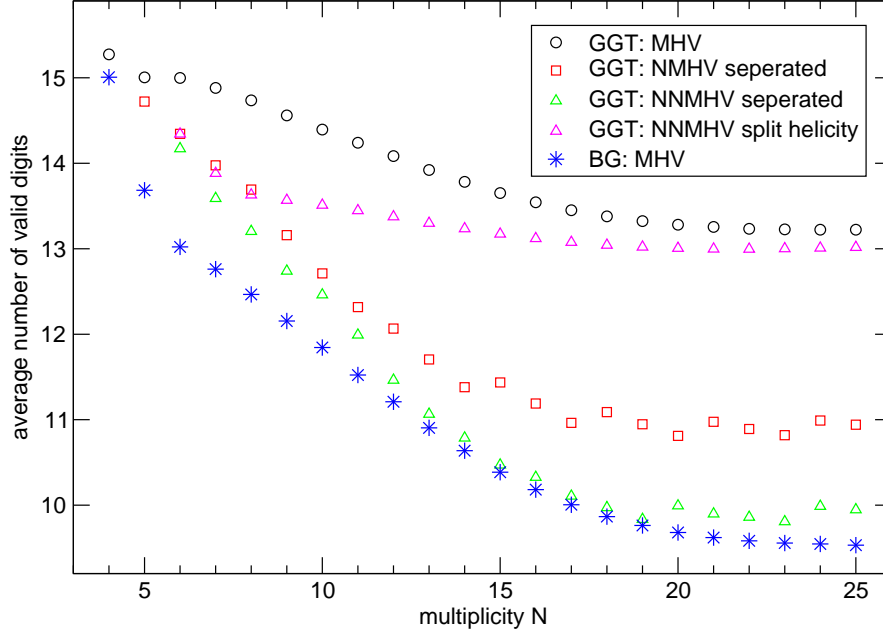


Figure 6: Average accuracy $|\delta|$ for pure gluon amplitudes as a function of the gluon multiplicity (GGT analytic formulae, BG Berends-Giele). Phase-space generation by sequential splitting.

vector the naive expectation would be that all helicity configurations should perform similar. A more detailed analysis shows a mild dependence on the helicity configuration as can be seen in Fig. 7. To assess the dependence of the aforementioned results on the phase space generation we show in Fig. 8 the average accuracy for a flat phase space generation obtained by using the algorithm RAMBO described in [19]. Comparing Fig. 7 and Fig. 8 we observe two important differences: First of all the dependence of the average accuracy on the helicity configuration is now more pronounced than in the case where collinear phase space configurations were preferred. Second we observe that in particular cases the accuracy can compete with the numerical evaluation using analytic formulae. Our understanding of the observed pattern is the following: Particular sub-amplitudes or even entire amplitudes may vanish due to “helicity conservation”. In the numerical approach this ‘zero’ is ‘calculated’ from a combination of individual non-zero contributions. Depending on the helicity configuration the cancellation may appear earlier or later in the recursion affecting through accumulated rounding errors the accuracy of the final result — leading to the observed helicity dependence of the average accuracy. In case that collinear phase space configurations are preferred a second effect becomes important: It is well known that scattering amplitudes in pure gauge theory show only square

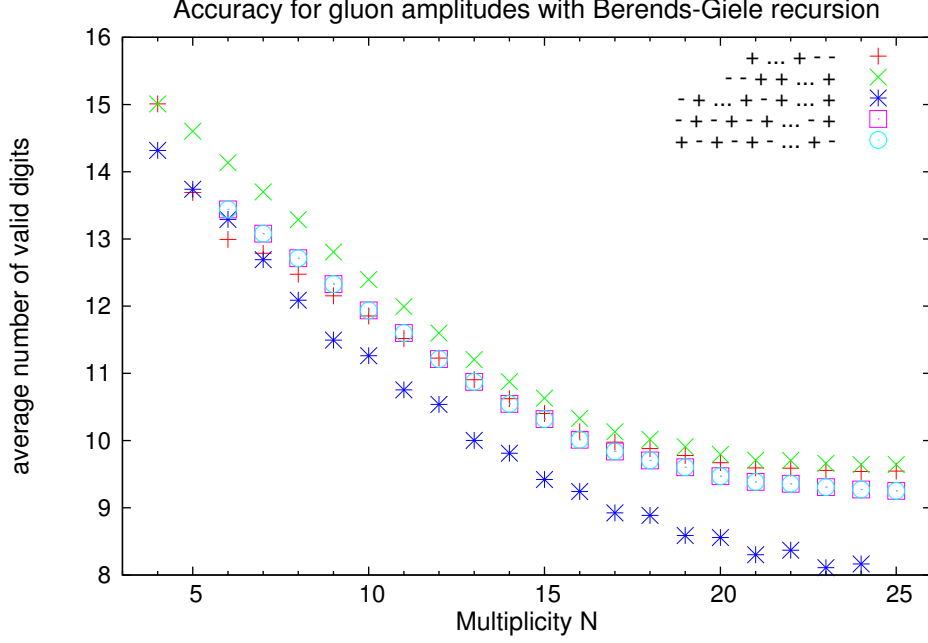


Figure 7: Average accuracy of the amplitude evaluation using Berends-Giele recursion for phase space generation with sequential splitting.

root singularities ($1/\sqrt{p_i p_j}$) for collinear phase space configurations ($p_i || p_j$). On the other hand individual Feynman diagrams show a more singular behavior. In the numerical approach the square root behavior is obtained through a numerical cancellation of the leading behavior. It is obvious that this leads to a loss of accuracy. In the extreme case for highly collinear configurations the 15 digits precision is no longer sufficient to evaluate a meaningful result. Using phase space configurations which tend to be collinear the second effect will dominate the average accuracy. As a consequence we observe in Fig. 7 only a mild dependence of the average accuracy for different helicity configurations together with an equally ‘bad’ overall accuracy. (One should keep in mind at this point that for all practical applications in collider phenomenology 8 significant digits are largely sufficient.) As far as the analytic formulae are concerned we observe an opposite effect: In case of a flat phase space generation no particular cancellation in the analytic formulae is present. As a consequence we observe a very high average accuracy close to the maximum of about 15 digits as one would have expected. However studying collinear configurations leads also in the analytic formulae to cancellations between individual terms. As a consequence the average accuracy degrades in that case.

One could argue that a flat phase space generation would be more appropriate to investigate the average accuracy. However we believe that for practical applications the average accuracy evaluated in that way would be less meaningful. In phenomenological applications the cross sections will get important contributions from collinear configurations. Using Monte Carlo methods for the cross section evaluation collinear events will thus dominate the total result. In an ideal situation this would be taken into account through the phase space integrator by pre-

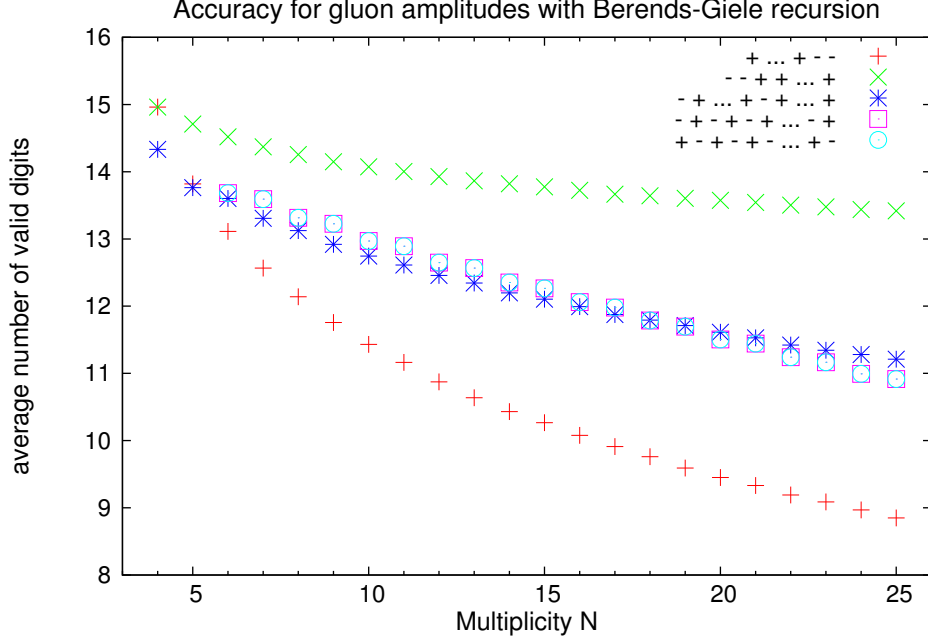


Figure 8: Average accuracy of the amplitude evaluation using Berends-Giele recursion for flat phase space generation.

ferring collinear configurations. This reasoning is also supported by the empirical observation that using RAMBO for the cross section evaluation usually leads to a poor performance of the Monte Carlo phase space integration in terms of computational effort and achieved integration accuracy.

For completeness we analyzed also the average accuracy for amplitudes involving massless quarks. The result is shown in Fig. 9. Again we have used a phase space generation preferring collinear events. As far as the numerical approach is concerned the result looks similar to the pure gluon case. This is just a consequence of the basic fact that the recurrence relation is very similar apart from the spin dependence. Since some vertices do not exist in the quark case the mixed amplitudes contain less terms and are slightly more precise. Concerning the analytic formulae we observe that the accuracy is not as good as in the pure gluon case. Our naive understanding is again that the corresponding formulae are more involved requiring more floating point evaluations and leaving more room for (unwanted) cancellations in the case of collinear phase space configurations.

4 Conclusions

QCD tree amplitudes are of great interest. The detailed analysis of their analytic structure may lead to a more profound understanding of $SU(N)$ gauge theories exposing further symmetries undiscovered so far. Concerning phenomenological applications tree amplitudes represent an important input for cross section evaluations in Born approximation and beyond. In this work

Numerical precision of quark amplitudes

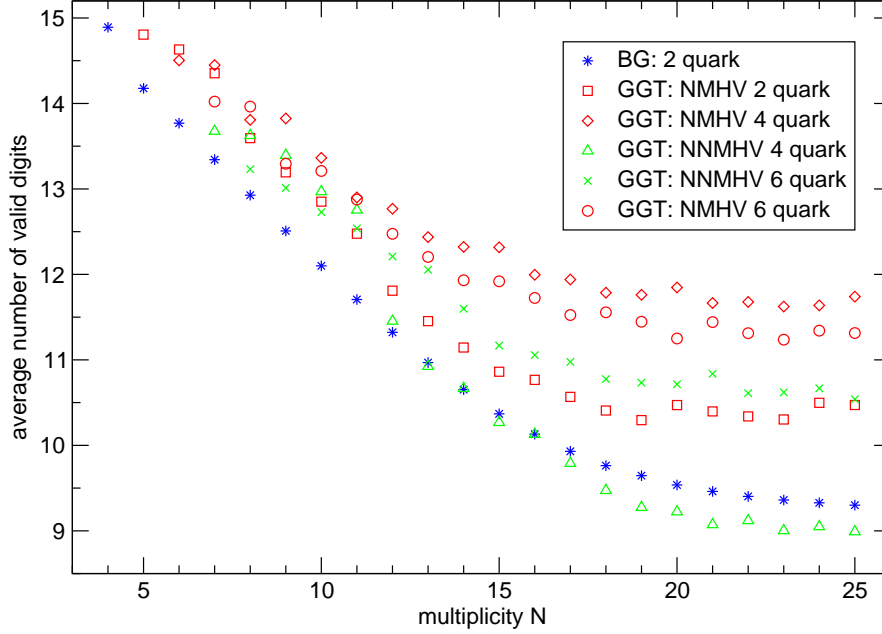


Figure 9: Average accuracy for amplitudes involving quarks. Phase-space generation by sequential splitting.

we have analyzed two different approaches to evaluate tree amplitudes. We have compared the numerical performance of a purely numerical approach based on the Berends-Giele recursion with the numerical evaluation of analytic formulae. In detail we find that MHV and NMHV amplitudes are most efficiently calculated using analytic formulae. For NNMHV amplitudes and beyond we find the purely numerical approach more efficient. We have also investigated the numerical accuracy. In general the numerical accuracy of the analytic formulae (evaluated numerically) is superior compared to the purely numerical approach. However we find that close to exceptional phase space configuration (soft/collinear configurations) analytic formulae suffer also from rounding errors. In both approaches we find even for large multiplicities an average accuracy of at least 9 digits—sufficient for phenomenological applications.

Acknowledgments

This work is supported in part by the Deutsche Forschungsgemeinschaft through the Transregional Collaborative Research Centre SFB-TR9 “Computational Particle Physics” and the Research Training Group (GK1504) “Mass, Spectrum, Symmetry, Particle Physics in the Era of the Large Hadron Collider” GK1504. In addition we gratefully acknowledge support from

the Helmholtz Alliance “*Physics at the Terascale*” contract VH-HA-101 and the Volkswagen Foundation.

References

- [1] T. Stelzer and W. Long, “*Automatic generation of tree level helicity amplitudes*”, Comput.Phys.Commun. 81, 357 (1994), hep-ph/9401258. • F. Krauss, R. Kuhn and G. Soff, “*AMEGIC++ 1.0: A Matrix element generator in C++*”, JHEP 0202, 044 (2002), hep-ph/0109036. • T. Gleisberg and S. Höche, “*Comix, a new matrix element generator*”, JHEP 0812, 039 (2008), arxiv:0808.3674.
- [2] Z. Bern, L. J. Dixon and D. A. Kosower, “*On-Shell Methods in Perturbative QCD*”, Annals Phys. 322, 1587 (2007), arxiv:0704.2798. • C. F. Berger and D. Forde, “*Multi-Parton Scattering Amplitudes via On-Shell Methods*”, Ann.Rev.Nucl.Part.Sci. 60, 181 (2010), arxiv:0912.3534. • R. Ellis, Z. Kunszt, K. Melnikov and G. Zanderighi, “*One-loop calculations in quantum field theory: from Feynman diagrams to unitarity cuts*”, arxiv:1105.4319, 157 pages, 20 figures, 580 equations. • H. Ita, “*Susy Theories and QCD: Numerical Approaches*”, J.Phys.A A44, 454005 (2011), arxiv:1109.6527.
- [3] S. Badger, B. Biedermann and P. Uwer, “*NGluon: A Package to Calculate One-loop Multi-gluon Amplitudes*”, Comput.Phys.Commun. 182, 1674 (2011), arxiv:1011.2900.
- [4] S. Becker, C. Reuschle and S. Weinzierl, “*Numerical NLO QCD calculations*”, JHEP 1012, 013 (2010), arxiv:1010.4187. • C. Berger et al., “*An Automated Implementation of On-Shell Methods for One-Loop Amplitudes*”, Phys.Rev. D78, 036003 (2008), arxiv:0803.4180. • G. Bevilacqua, M. Czakon, M. Garzelli, A. van Hameren, A. Kardos et al., “*HELAC-NLO*”, arxiv:1110.1499. • F. Cascioli, P. Maierhofer and S. Pozzorini, “*Scattering Amplitudes with Open Loops*”, Phys.Rev.Lett. 108, 111601 (2012), arxiv:1111.5206. • G. Cullen, N. Greiner, G. Heinrich, G. Luisoni, P. Mastrolia et al., “*Automated One-Loop Calculations with GoSam*”, Eur.Phys.J. C72, 1889 (2012), arxiv:1111.2034. • W. Giele and G. Zanderighi, “*On the Numerical Evaluation of One-Loop Amplitudes: The Gluonic Case*”, JHEP 0806, 038 (2008), arxiv:0805.2152. • W. Giele, Z. Kunszt and J. Winter, “*Efficient Color-Dressed Calculation of Virtual Corrections*”, Nucl.Phys. B840, 214 (2010), arxiv:0911.1962. • V. Hirschi, R. Frederix, S. Frixione, M. V. Garzelli, F. Maltoni et al., “*Automation of one-loop QCD corrections*”, JHEP 1105, 044 (2011), arxiv:1103.0621. • A. Lazopoulos, “*Multi-gluon one-loop amplitudes numerically*”, arxiv:0812.2998.
- [5] Z. Bern, G. Diana, L. Dixon, F. Febres Cordero, S. Hoeche et al., “*Four-Jet Production at the Large Hadron Collider at Next-to-Leading Order in QCD*”, arxiv:1112.3940. • C. Berger et al., “*Precise Predictions for $W + 4$ Jet Production at the Large Hadron Collider*”, arxiv:1009.2338. • H. Ita, Z. Bern, L. Dixon, F. Febres Cordero, D. Kosower et al., “*Precise Predictions for $Z + 4$ Jets at Hadron Colliders*”, Phys.Rev. D85, 031501 (2012), arxiv:1108.2229. • A. Bredenstein, A. Denner, S. Dittmaier and S. Pozzorini, “*NLO QCD corrections to $pp \rightarrow t$ anti- t b anti- b + X at the LHC*”, Phys.Rev.Lett. 103, 012002 (2009), arxiv:0905.0110. • A. Denner, S. Dittmaier, S. Kallweit and S. Pozzorini, “*NLO QCD corrections to $WWbb$ production at hadron colliders*”, Phys.Rev.Lett. 106, 052001 (2011), arxiv:1012.3975. • R. Frederix, S. Frixione, K. Melnikov and G. Zanderighi, “*NLO QCD corrections to five-jet production at LEP and the extraction of $\alpha_s(M_Z)$* ”,

- JHEP 1011, 050 (2010), arxiv:1008.5313. • S. Becker, D. Goetz, C. Reuschle, C. Schwan and S. Weinzierl, “*NLO results for five, six and seven jets in electron-positron annihilation*”, Phys.Rev.Lett. 108, 032005 (2012), arxiv:1111.1733. • N. Greiner, G. Heinrich, P. Mastrolia, G. Ossola, T. Reiter et al., “*NLO QCD corrections to the production of $W^+ W^-$ plus two jets at the LHC*”, arxiv:1202.6004. • N. Greiner, A. Guffanti, T. Reiter and J. Reuter, “*NLO QCD corrections to the production of two bottom-antibottom pairs at the LHC*”, Phys.Rev.Lett. 107, 102002 (2011), arxiv:1105.3624. • G. Bevilacqua, M. Czakon, C. Papadopoulos and M. Worek, “*Hadronic top-quark pair production in association with two jets at Next-to-Leading Order QCD*”, Phys.Rev. D84, 114017 (2011), arxiv:1108.2851. • G. Bevilacqua, M. Czakon, C. Papadopoulos, R. Pittau and M. Worek, “*Assault on the NLO Wishlist: $pp \rightarrow t \bar{t} \text{ anti-}t \bar{b} \text{ anti-}b$* ”, JHEP 0909, 109 (2009), arxiv:0907.4723. • G. Bevilacqua, M. Czakon, A. van Hameren, C. G. Papadopoulos and M. Worek, “*Complete off-shell effects in top quark pair hadroproduction with leptonic decay at next-to-leading order*”, JHEP 1102, 083 (2011), arxiv:1012.4230. • G. Bozzi, F. Campanario, M. Rauch and D. Zeppenfeld, “ *$Z\gamma\gamma$ production with leptonic decays and triple photon production at NLO QCD*”, Phys.Rev. D84, 074028 (2011), arxiv:1107.3149. • F. Campanario, C. Englert, M. Rauch and D. Zeppenfeld, “*Precise predictions for $W\gamma\gamma$ +jet production at hadron colliders*”, Phys.Lett. B704, 515 (2011), arxiv:1106.4009. • K. Arnold, J. Bellm, G. Bozzi, M. Brieg, F. Campanario et al., “*VBFNLO: A parton level Monte Carlo for processes with electroweak bosons – Manual for Version 2.5.0*”, arxiv:1107.4038. • S. Becker, C. Reuschle and S. Weinzierl, “*Efficiency improvements for the numerical computation of NLO corrections*”, arxiv:1205.2096. • R. K. Ellis, K. Melnikov and G. Zanderighi, “ *$W+3$ jet production at the Tevatron*”, Phys.Rev. D80, 094002 (2009), arxiv:0906.1445. • R. Frederix, S. Frixione, V. Hirschi, F. Maltoni, R. Pittau et al., “*aMC@NLO predictions for Wjj production at the Tevatron*”, JHEP 1202, 048 (2012), arxiv:1110.5502. • T. Melia, K. Melnikov, R. Rontsch and G. Zanderighi, “*Next-to-leading order QCD predictions for W^+W^+jj production at the LHC*”, JHEP 1012, 053 (2010), arxiv:1007.5313. • T. Melia, K. Melnikov, R. Rontsch and G. Zanderighi, “*NLO QCD corrections for W^+W^- pair production in association with two jets at hadron colliders*”, Phys.Rev. D83, 114043 (2011), arxiv:1104.2327.
- [6] R. Britto, F. Cachazo and B. Feng, “*New recursion relations for tree amplitudes of gluons*”, Nucl. Phys. B715, 499 (2005), hep-th/0412308. • R. Britto, F. Cachazo, B. Feng and E. Witten, “*Direct proof of tree-level recursion relation in Yang-Mills theory*”, Phys. Rev. Lett. 94, 181602 (2005), hep-th/0501052.
- [7] N. Arkani-Hamed, F. Cachazo, C. Cheung and J. Kaplan, “*A Duality For The S Matrix*”, JHEP 1003, 020 (2010), arxiv:0907.5418.
- [8] J. M. Drummond and J. M. Henn, “*All tree-level amplitudes in $\mathcal{N}=4$ SYM*”, JHEP 0904, 018 (2009), arxiv:0808.2475.
- [9] L. J. Dixon, J. M. Henn, J. Plefka and T. Schuster, “*All tree-level amplitudes in massless QCD*”, JHEP 1101, 035 (2011), arxiv:1010.3991.
- [10] J. L. Bourjaily, “*Efficient Tree-Amplitudes in $N=4$: Automatic BCFW Recursion in Mathematica*”, arxiv:1011.2447.
- [11] M. Dinsdale, M. Ternick and S. Weinzierl, “*A Comparison of efficient methods for the computation of Born gluon amplitudes*”, JHEP 0603, 056 (2006), hep-ph/0602204. • C. Duhr, S. Hoeche and F. Maltoni, “*Color-dressed recursive relations for multi-parton amplitudes*”, JHEP 0608, 062 (2006), hep-ph/0607057.

- [12] W. Giele, G. Stavenga and J.-C. Winter, “*Thread-Scalable Evaluation of Multi-Jet Observables*”, Eur.Phys.J. C71, 1703 (2011), [arxiv:1002.3446](#). • K. Hagiwara, J. Kanzaki, N. Okamura, D. Rainwater and T. Stelzer, “*Calculation of HELAS amplitudes for QCD processes using graphics processing unit (GPU)*”, Eur.Phys.J. C70, 513 (2010), [arxiv:0909.5257](#).
- [13] M. L. Mangano and S. J. Parke, “*Multi-Parton Amplitudes in Gauge Theories*”, Phys. Rept. 200, 301 (1991), [hep-th/0509223](#).
- [14] S. J. Parke and T. R. Taylor, “*An Amplitude for n Gluon Scattering*”, Phys. Rev. Lett. 56, 2459 (1986).
- [15] F. A. Berends and W. T. Giele, “*Recursive Calculations for Processes with n Gluons*”, Nucl. Phys. B306, 759 (1988).
- [16] L. J. Dixon, “*Calculating scattering amplitudes efficiently*”, [hep-ph/9601359](#).
- [17] S. Badger, B. Biedermann and P. Uwer, “*One-Loop Amplitudes for Multi-Jet Production at Hadron Colliders*”, [arxiv:1201.1187](#).
- [18] E. Byckling and K. Kajantie, “*Particle kinematics*”, Wiley (1973).
- [19] R. Kleiss, W. J. Stirling and S. Ellis, “*A new Monte Carlo treatment of multiparticle phase space at high-energies*”, Comput.Phys.Commun. 40, 359 (1986).